Jurnal Teknologi

Full Paper

EFFECT OF PMMA-MWNTS LOADING ON CO_2 SEPARATION PERFORMANCE OF THIN FILM NANOCOMPOSITE MEMBRANE

Wong Kar Chun, Goh Pei Sean*, Ahmad Fauzi Ismail

Advanced Membrane Technology Research Centre, Faculty of Chemical and Energy Engineering, Universiti Teknologi Malaysia, 81310, Johor, Malaysia

*Corresponding author
peisean@petroleum.utm.my

Article history
Received
26 August 2016
Received in revised form
31 October 2016
Accepted
1 November 2016

Graphical abstract

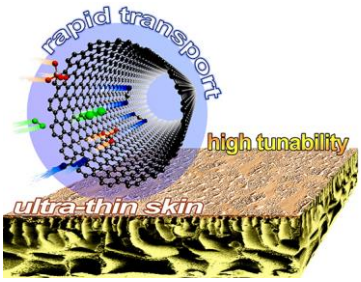

Abstract

Nanocomposite membrane, especially the thin film nanocomposite (TFN) fabricated via interfacial polymerization (IP) is a relatively new class of membrane which features good separation performance and practical processing. This study investigated on the effects of multi-walled carbon nanotubes (MWNTs) loading on the gas separation performance of the resultant TFNs. TFNs were tested with pure CO_2, N_2 and CH_4 gases at feed pressure of 2 bar. The findings from this study suggested that the optimum fillers loading was around 0.25 g/L in the coating solution which gives TFN with CO_2 permeance of 53.5 gas permeation unit (GPU) (12% higher than base membrane without filler), CO_2/N_2 selectivity of 61 and CO_2/CH_4 selectivity of 35. The enhancement in CO_2 permeance without sacrificing the membrane selectvities was attributed to the good dispersion and compatibility of the MWNTs with the polymer matrix while the nanotubes serve as rapid diffusion channels to facilitate transport of gases. TFN embedded with polymethyl methacrylate (PMMA)-MWNTs showed potential for low pressure carbon capture and storage application.

Keywords: Thin film nanocomposite, interfacial polymerization, multi-walled carbon nanotubes

Abstrak

Membran nanokomposit terutamanya nanokomposit filem nipis (TFN) yang difabrikasi melalui pempolimeran antara muka (IP) merupakan kelas membran baru yang bercirikan prestasi pemisahan yang baik dan pemprosesan yang praktikal. Kajian ini telah menyiasat kesan-kesan daripada perubahan muatan tiub-tiub nano karbon berbilang dinding (MWNTs) terhadap prestasi permisahan gas oleh TFNs yang terhasil. TFNs telah diuji menggunakan gas CO_2, N_2 dan CH_4 yang tulen pada tekanan suapan sebanyak 2 bar. Penemuan daripada kajian ini mencadangkan bahawa muatan pengisi yang optimum adalah disekitar 0.25 g/L di dalam larutan penyalut yang memberikan TFN berketelapan CO_2 sebanyak 53.5 unit telapan gas (GPU) (12% lebih tinggi berbanding membran tanpa pengisi), kememilihan CO_2/N_2 sebanyak 61 dan kememilihan CO_2/CH_4 sebanyak 35. Peningkatan telapan CO_2 tanpa mengorbankan kememilihan membrane adalah disebabkan penyebaran yang baik dan keserasian MWNTs dengan matriks polimer sementara tiub-tiub nano ini berfungsi sebagai saluran resapan yang pantas untuk memudahkan pengangkutan gas-gas. TFN yang mengandungi polimetil metakrilat (PMMA)-MWNTs telah menunjukkan potensi untuk aplikasi pengumpulan dan penyimpanan karbon pada tekanan rendah.

Kata kunci: Nanokomposit filem nipis, pempolimeran antara muka, tiub-tiub nano karbon berbilang dinding

1.0 INTRODUCTION

Over the past decades, the impacts of greenhouse effect resulted from unregulated emission of excessive carbon dioxide (CO_2) have been felt across the globe. In view of the severity of this issue, implementation of environmental protection and energy policies has been strengthened to control the release of greenhouse gases and reduce fossil fuels consumption. Meanwhile, separation at source is deemed as a viable approach to keep the atmospheric CO_2 concentration in check and membrane is a well-suited candidate for this application. Membrane separation is not only energy efficient and environmental friendly, its design simplicity and compactness ensure hassle-free operation [1, 2].

Thin film composite (TFC) fabricated via interfacial polymerization (IP) is a wonderful class of membrane which features ultrathin active layer, flexible tunability and ease of upscaling [3–5]. By incorporating inorganic nanoparticles into the composite matrix to produce thin film nanocomposite (TFN), the membrane performance can be significantly improved to overcome the permeance-selectivity trade-off of polymeric material [6–8]. In recent year, the preference on filler has shifted from metal-based to carbon-based material due to the vast availability of carbon sources for sustainable development. Carbon-based filler especially the carbon nanotube (CNT) exhibits good chemical, thermal stability and mechanical properties which can improve the overall durability of the host composite [9–11]. Additionally, attributed to the smooth graphitic wall of CNT, it has been reported that gases could utilize the CNT pores as rapid diffusion channels leading to high membrane permeability [12–14]. However, fabricating a defect-free CNT composite is often a challenge because this nanotube has very high surface area to volume ratio which makes them easily entangled with one another forming undesirable aggregates [15–17]. Furthermore, the disparity of its properties from the polymeric matrix presents severe incompatibility issue which leads to the formation of filler-matrix interfacial voids and adversely impacts membrane selectivity [18, 19].

Our previous works [20,21] demonstrated that grafting the multi-walled carbon nanotube (MWNT) with polymethyl methacrylate (PMMA) can tackle both the dispersibility and compatibility issues while the employment of ball milling modification can suppress MWNT aggregation. Additionally, our strategy of embedding the nanofillers within the intermediate layer between support and active skin layers has proven to be effective in minimizing MWNT protrusion. Since the extent of performance enhancement is directly related to the content of nanofillers while the capacity of the polymeric matrix to host the nanofillers are critically influenced by the nature of fillers and fabrication technique used, it is important to identify the optimal PMMA-MWNT loading that can be embedded into the TFN. Hence, in this study, the effects of PMMA-MWNT loading on the formation of polyamide (PA) thin film and gas separation performance were investigated.

2.0 METHODOLOGY

2.1 Materials

The materials used in this study include MWNTs (98 % carbon basis, OD × ID × L: 10 ± 1 nm × 4.5 ± 0.5 nm × 3-6 μm), polyvinylpyrrolidone (PVP, K90) and diethylene glycol bis(3-aminopropyl) ether (DGBAmE, 97 %) purchased from Sigma Aldrich, sulfuric acid (H_2SO_4, 95-97 %), nitric acid (HNO_3, 65 %), methyl methacrylate (MMA), N-methyl-2-pyrrolidone (NMP, 99 %), n-hexane (99 %), potassium persulfate (KPS), sodium hydrogen carbonate ($NaHCO_3$) and sodium carbonate (Na_2CO_3 purchased from Merck, cetyltrimethyammonium bromide (CTAB, 99 %) and trimesoyl chloride (TMC, 98%) from Acros Organics, methanol (99.8 %) and ethanol (96 %) from Fisher Scientific, polydimethylsiloxane (PDMS, Sylgard 184, Dow Corning) and polysulfone (PSf, Udel P-3500, Solvay).

2.2 Synthesis of PMMA-MWNTs

2.0 g of MWNTs was added into 400 mL of H_2SO_4:HNO_3 (3:1v/v, each 3 M) mixed acids solution at 80 °C for 6 h to oxidize the nanotubes. Then the dispersion solution was filtered. The MWNTs residue was rinsed with deionized (DI) water until pH 6 before rinsed with 400 mL of ethanol and left to dry overnight at 60 °C. Next, 1.5 g of the oxidized MWNTs was mixed with 10 g of CTAB, 10 g of MMA and 300 mL of DI water followed by 20 min ultrasonication. The solution was then poured into a 500 mL three-neck round bottom flask that was equipped with a condenser, a mechanical stirrer and a nitrogen inlet and placed in a 70 °C oil bath. The air in the flask was replaced by a stream of nitrogen and the mixture was stirred at 500 rpm. 3 g of KPS and 2 g of $NaHCO_3$ were gradually added into the mixture and the reaction was allowed to take place for 21 h with continuous stirring until a grayish odorless solution was produced. The latex dispersion was drawn out from the flask and added into methanol solution before allowed to stand overnight. After that, the precipitant was filtered via vacuum filtration and washed with excess methanol and DI water before dried in oven at 60 °C. Finally, 1 g of PMMA grafted MWNTs were ball-milled in a 100 mL Scott bottle containing ≈ 200 g of 1/4 in steel balls for 8 h using a bench-top laboratory roller mill. The final product was desiccated and kept in a 20 mL glass vial until used for fabricating TFN.

2.3 Fabrication of PSF Supports

PSf (15 wt. %) and PVP (3 wt. %) were dissolved in NMP (82 wt. %) with stirring until a viscous solution was obtained. The dope solution was casted on a clean glass plate using a glass roller and immediately immersed into coagulation bath (water) at room temperature and allowed to sit for 10 min to ensure a complete phase inversion process. The thickness of the PSf support was controlled by the cellulose tapes (3 layers each) that were taped at the two opposing ends of the glass plate. After that, the fabricated PSf membrane was peeled and stored in a fresh DI water for 24 h to remove residue solvent. All supports were post-treated in ethanol solutions for 5 min followed by n-hexane for 1 min before left to dry at ambient condition for 12 h. Dried PSf supports were kept in air-tight plastic bags until used for fabricating TFN

2.4 Fabrication of TFNs

The active surface of PSf support was coated with a 2 wt. % PDMS solution containing PMMA-MWNTs (0.00 g/L, 0.05 g/L, 0.25 g/L, 0.5 g/L and 1.0 g/L) using n-hexane as solvent for 10 min then dried in ambient condition for 12 h. Coated PSf support was sandwiched in between a glass plate (bottom) and Viton rubber frame (top) to be impregnated with organic phase of 0.28 % w/v TMC in n-hexane for 10 min. Excess solution was carefully removed from the surface before polymerizing the impregnated support with aqueous phase containing 0.35 % w/v DGBAmE and 0.4 % w/v Na_2CO_3 for 3 min to form the PA thin film. The resultant composite membrane was dried in ambient condition for 12 h. Composite membrane without nanotubes was dubbed TFC while those containing PMMA-MWNTs were denoted as TFN-X where X indicates the filler loading (e.g. composite fabricated using PSf coated with PDMS solution containing 0.5 g/L PMMA-MWNTs was denoted as TFN-0.5). All solutions containing nanofillers were sonicated for 1 h before used.

2.5 Characterization of PMMA-MWNTS and TFNS

Fourier transform infrared spectroscopy (FTIR, Nicolet 5700, Thermo Electron Corporation) was used to identify the functional groups present in nanotubes and TFNs. Thermogravimetric analysis (TGA, DSC822^e, Mettler Toledo) conducted in the temperature range of 25 °C - 600 °C and under nitrogen gas flow at heating rate of 10 °C/min was used to determine the degree of PMMA grafting while transmission electron microscopy (TEM, HT7700, Hitachi) was used to inspect the structure of MWNTs. The surface and cross section morphologies of the fabricated membranes were investigated using field emission scanning electron microscopy (FESEM, SU8020, Hitachi). For cross section scan, the samples were fractured in liquid nitrogen to obtain a clean break so that the original morphologies were retained.

2.6 Gas Permeation Test

The permeance of pure (N_2), methane (CH_4) and CO_2
across the membranes were determined by variable volume method using a simple soap bubble meter with 2 bar feed pressure at room temperature while the outlet stream was exposed to atmospheric conditions. Circular membrane disc with effective permeation area of 13.5 cm^2 was used. Upstream of the membrane chamber was always purged with the test gas prior to permeation measurement. The gas permeance reading was taken after a steady state was reached and the average of three replicates was used to represent each set of data. Gas permeance was determined using the following expression:

$$(P/l)_i = Q_i / (\Delta p \cdot A)$$

Where, Q_i is the volumetric flow rate of gas '*i*' ($cm^3\ s^{-1}$) at standard temperature and pressure, *l* is the membrane thickness (cm), A is the effective membrane area (cm^2) and Δp is the trans-membrane pressure difference (cmHg). Permeances are expressed in gas permeation units (GPU) where:

1 GPU = 1 × 10^{-6} cm^3 (STP) $(cm^2 \cdot s \cdot cmHg)^{-1}$

The pure gas selectivity was obtained by taking the ratio of the pure gas permeabilities:

$$\alpha_j^i = (P/l)_i / (P/l)_j$$

3.0 RESULTS AND DISCUSSION

3.1 Characterization of MWNTS

As depicted in Figure 1, all the spectra indicate the presence of hydroxyl groups in all the MWNTs attributed by the broad absorption bands around 3200 cm^{-1} and 3600 cm^{-1} of the -OH stretching. For PMMA-MWNTs, the detection of absorption peak of carbonyl groups (C=O) at 1726 cm^{-1} and peaks of C-O stretching at 1156 cm^{-1} and 1046 cm^{-1} which are not present in pristine MWNTs provide indication that PMMA has been successfully grafted on the nanotube surface [22, 23].

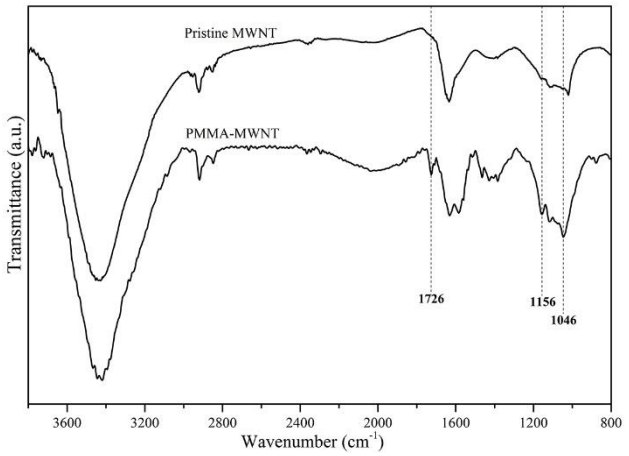

Figure 1 FTIR spectra of pristine MWNT and PMMA-MWNT

Based on Figure 2, at decomposition temperature below 600 °C, the pristine MWNTs experienced a minute mass loss of about 2 % due to the breakdown of carboxylic (-COO) and hydroxyl (-OH) groups whereas the oxidized sample undergone about 6 % loss in mass This is a good indication that the acid oxidation process was successfully carried out and the introduction of functional groups into the MWNTs structure slightly reduce their thermal property [24]. The mass of PMMA-MWNTs sample decreased rapidly from 200 °C to 480 °C due to the decomposition of grafted PMMA. Based on the difference in mass loss between PMMA-MWNTs and oxidized MWNTs within the 200 - 480 °C range, PMMA grafting degree was estimated to be around 16.6%.

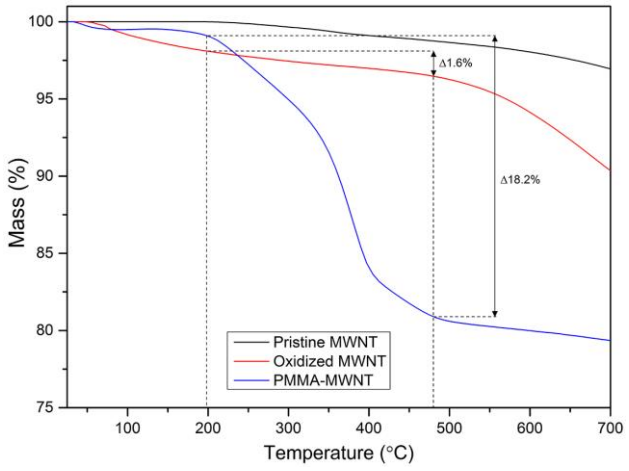

Figure 2 TGA profiles of pristine MWNTs, O-MWNTs and PMMA-MWNTs

TEM analysis was performed to evaluate the extent of the nanotube structural changes and the results are presented in Figure 3. TEM image of pristine MWNT (Figure 3b) reveals that the nanotube was close-ended (indicated by red arrow) and impurity such as metal-catalyst (indicated by red circle) was present. After modification, the nanotube tip was completely opened (indicated by blue arrow in Figure 3d) while no impurities can be observed. Tip opening is important as this allows gases to utilize the MWNTs pore as diffusion channels whereas the removal of impurities ensures the transport of gases is not obstructed. These changes were typically achieved during the oxidation step whereby the harsh acidic environment dissolved all the metal catalysts and digested the loose amorphous carbon as well as thin carbon wall [25,26]. Although it has been reported that prolong oxidation can destroy the MWNTs, overall, the structural integrity of modified nanotubes in this study was retained with no visible wall damages (compare Figure 3a and Figure 3c).

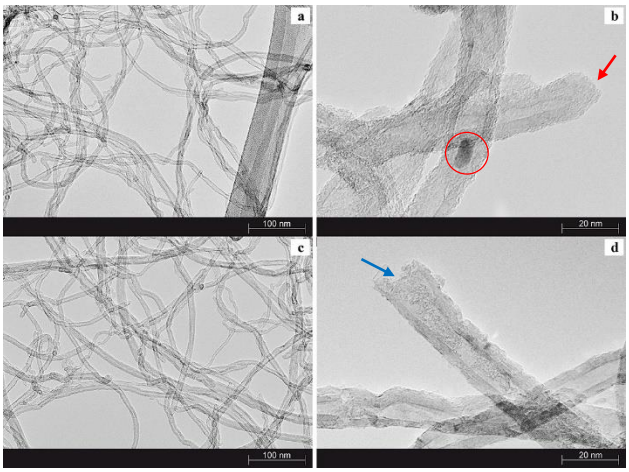

Figure 3 TEM images of (a and b) pristine MWNTs and (c and d) PMMA-MWNTs at ×120k and ×600k magnification respectively

3.2 Characterization of TFNS

FTIR spectra of all the composite membranes in Figure 4 show that interfacial polymerization has successfully taken place since strong characteristic peaks of C=O (amide I) at 1655 cm^{-1}, N-H (amide II) at 1543 cm^{-1} and C-N at 1243 cm^{-1} which correspond to the amide groups formed during IP were detected. Moreover, all the spectra of TFN is identical to that of TFC, despite PMMA-MWNTs were added, which suggested that the nanofillers were well-encapsulated within the PDMS coating layer which masked their IR signatures.

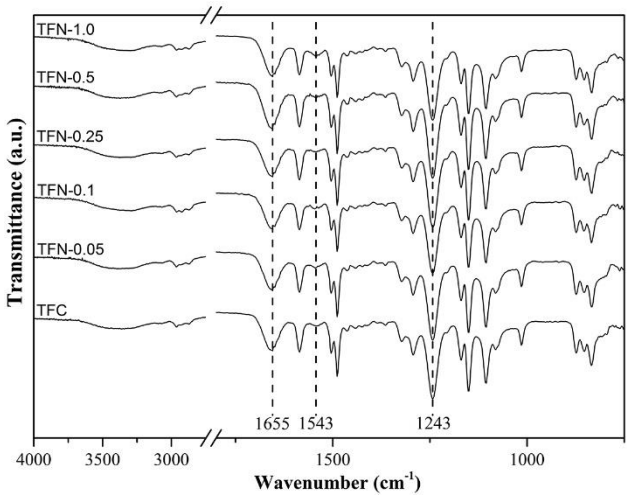

Figure 4 ATR-FTIR spectra of TFNs with different loading

The structure and integrity of the PA layer were further examined via FESEM. Figure 5 shows the cross sections of the TFNs containing different MWNTs loading and all samples have PA skin layer with thickness around 185 ± 15 nm. On the other hand, Figure 6 reveals that content of embedded fillers has a direct impact on the PA surface structure in which the nodules size monotonously increased with PMMA-MWNTs loading. Furthermore, the incorporation of PMMA grafted nanotubes has led to formation of more interconnected nodules (leaf-like structure) whereas the nodules in TFC are distinct and distance from one another.

Addition of PMMA-MWNTs introduced polar functional groups (C=O, -OH) onto the surface of coated support which diminished the hydrophobic characteristic of PDMS-treated support layer and improves wettability by aqueous solution. Furthermore, the presence of polar groups is known to attract amine [27]. Hence, higher PMMA-MWNTs content induces more amine to diffuse into the reaction zone, yielding greater PA mass (larger nodule) when the TMC-impregnated support was brought into contact with the aqueous phase during IP. Similar trend was also observed in the works by Ghosh *et al.* [28] and Barona *et al.* [29] who described the morphological change as result of increased miscibility between the aqueous phase and organic phase. Overall, composite samples with filler loading less than 0.5 g/L exhibited good nodules dispersion which fully cover the support surface. However, beyond the 0.5 g/L threshold, coarse structures began to form which has detrimental effects on the nodules dispersion or coverage. The nanotubes tend to cluster into large aggregates at high loading. Our previous work has demonstrated that, PMMA-MWNTs can form linkages with PDMS chains [20]. Greater extend of clustering allows more PDMS linkages to form and resulted in the formation of dense impermeable structures.

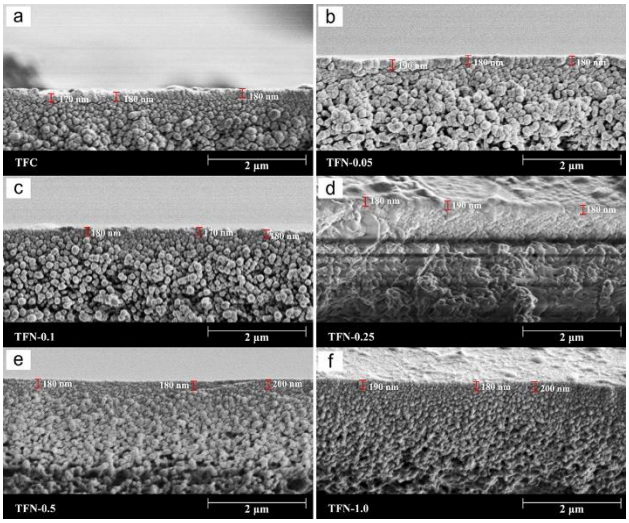

Figure 5 Cross sections of (a) TFC and TFN loaded with (b) 0.05 g/L, (c) 0.1 g/L, (d) 0.25 g/L, (e) 0.5 g/L and (f) 1.0 g/L of PMMA-MWNTs obtained using FESEM at ×20k magnification

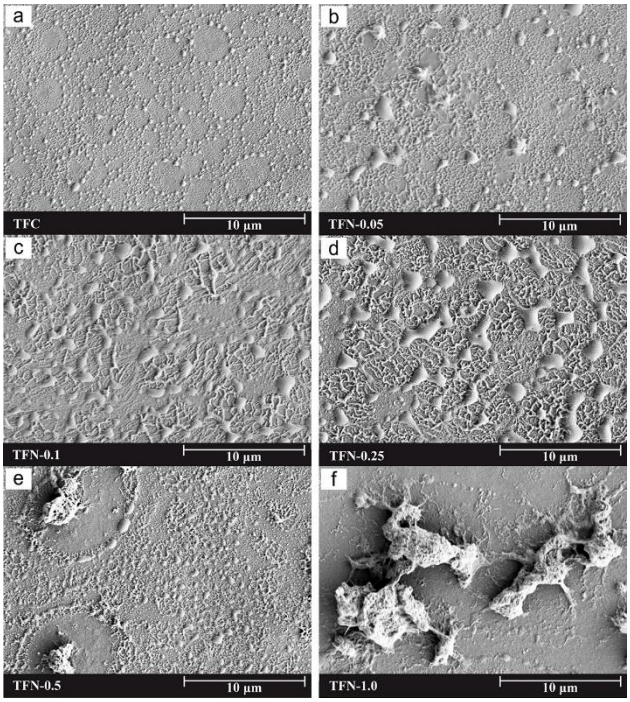

Figure 6 Surface morphologies of (a) TFC and TFN loaded with (b) 0.05 g/L, (c) 0.1 g/L, (d) 0.25 g/L, (e) 0.5 g/L and (f) 1.0 g/L of PMMA-MWNTs obtained using FESEM at ×5k magnification

3.3 Gas Separation Performance of TFNS

Based on results from gas permeation test depicted in Figure 7, the CO_2 permeance increased as the loading of the modified nanotubes raised from 0.05 g/L to 0.25 g/L. Similar enhancement in fluid transport rate when nanotubes loading was increased has also been reported elsewhere [30–32]. At low fillers

loading (<0.25 g/L), the improvement in CO_2 transport rate was well-attributed to the increased in nanotubes content within the TFN which provided more rapid diffusion channels to facilitate mass transport of the gases [33]. Besides, the nanotubes were well-dispersed which enables the formation of defect-free selective thin film.

On the contrary, when TFN was overloaded with fillers (>0.5 g/L), aggregation of nanotubes negatively impacted the permeation of gases. Aggregation diminished the functionality of embedded PMMA-MWNTs as diffusion channels because the nanofillers are constrained within balls of compact structures and the gases were forces to travel around these impermeable nanotube-polymer aggregates. Since the aggregates size increases with nanofillers content, eventually, the large aggregates clogged the pores of support layer resulting in TFN-1.0 CO_2 permeance that is lower than that of the control membrane (TFC).

The variation in PMMA-MWNTs loading does not seems to has significant effect on TFN selectivity. Since the MWNTs used in this experiment have internal diameter (4.5 nm or 45 Å) which is 10 times bigger than the kinetic diameter of the biggest test gas (CH_4 = 3.8 Å, N_2, 3.64 Å, CO_2 = 3.3 Å [34]), the nanofillers possess no size-exclusion property. As such, all test gases benefitted equally from the MWNTs addition which resulted in constant CO_2/N_2 and CO_2/CH_4 selectivities.

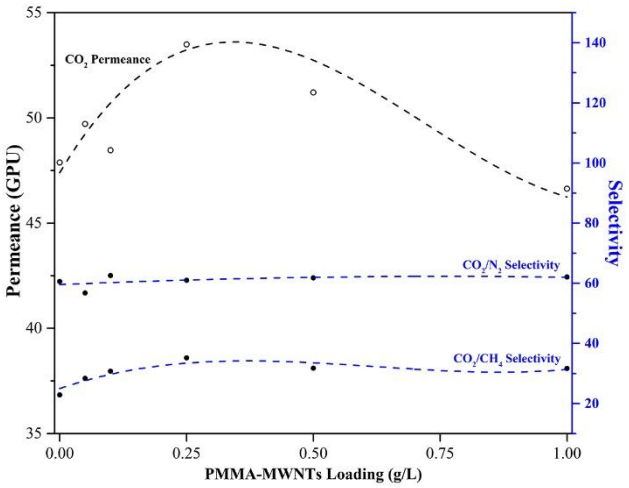

Figure 7 Gas separation performance of different gases through the resultant TFNs with different PMMA-MWNTs loadings

4.0 CONCLUSION

Overall, this study demonstrated that the content of nanofiller embedded into the TFN greatly affects the surface morphologies of the PA thin film layer and separation performance of the membrane. While addition a low amount of PMMA-MWNTs enhanced the CO_2 permeance, overloading the TFN has deteriorated the membrane performance. In this study, the optimum PMMA-MWNTs loading lies between 0.25 g/L to 0.5 g/L while our best sample (TFN-0.25) gives CO_2 permeance of 53.5 GPU (12% increment), CO_2/N_2 selectivity of 61 and CO_2/CH_4 selectivity of 35.

Acknowledgement

Authors would like to acknowledge the financial support provided by Flagship Grant Scheme from Universiti Teknologi Malaysia (03G43) and Higher Institution Centre of Excellence (HICOE) Research Grant Scheme from Ministry of Education Malaysia (4J183).

References

[1] Sanders, D. F., Smith, Z. P., Guo, R., Robeson, L. M., McGrath, J. E., Paul, D. R., & Freeman, B. D. 2013. Energy-Efficient Polymeric Gas Separation Membranes For A Sustainable Future: A Review. *Polymer*. 54: 4729-4761.

[2] Goh, P. S. & Ismail, A. F. 2015. Graphene-based Nanomaterial: The State-Of-The-Art Material For Cutting Edge Desalination Technology. *Desalination*. 356: 115-128.

[3] Sorribas, S., Gorgojo, P., & Livingston, A.G. 2013. High Flux Thin Film Nanocomposite Membranes Based on Metal − Organic Frameworks for Organic Solvent Nano filtration. *Journal of The American Chemical Society*. 135(40): 15201-15208.

[4] Yu, X., Wang, Z., Zhao, J., Yuan, F., Li, S., Wang, J., & Wang, S. 2011. An Effective Method to Improve the Performance of Fixed Carrier Membrane via Incorporation of CO2-selective Adsorptive Silica Nanoparticles. *Chinese Journal of Chemical Engineering*. 19: 821-832.

[5] Yu, X., Wang, Z., Wei, Z., Yuan, S., Zhao, J., Wang, J., & Wang, S. 2010. Novel Tertiary Amino Containing Thin Film Composite Membranes Prepared By Interfacial Polymerization For CO2 Capture. *Journal of Membrane Science*. 362: 265-278.

[6] De Sitter, K., Dotremont, C., Genné, I., & Stoops, L. 2014. The Use Of Nanoparticles As Alternative Pore Former For The Production Of More Sustainable Polyethersulfone Ultrafiltration Membranes. *Journal of Membrane Science*. 471: 168-178.

[7] Ahmad, A. L., Jawad, Z. A., Low, S. C., & Zein, S. H. S. 2014. A Cellulose Acetate/Multi-Walled Carbon Nanotube Mixed Matrix Membrane For CO2/N2 Separation. *Journal of Membrane Science*. 451: 55-66.

[8] Lua, A. C. & Shen, Y. 2013. Preparation And Characterization Of Polyimide-Silica Composite Membranes And Their Derived Carbon-Silica Composite Membranes For Gas Separation. *Chemical Engineering Journal*. 220: 441-451.

[9] Aroon, M. A., Ismail, A. F., Montazer-Rahmati, M. M., & Matsuura, T. 2010. Effect Of Chitosan As A Functionalization Agent On The Performance And Separation Properties Of Polyimide/Multi-Walled Carbon Nanotubes Mixed Matrix Flat Sheet Membranes. *Journal of Membrane Science*. 364: 309-317.

[10] Sanip, S. M., Ismail, A. F., Goh, P. S., Soga, T., Tanemura, M., & Yasuhiko, H. 2011. Gas Separation Properties Of Functionalized Carbon Nanotubes Mixed Matrix Membranes. *Separation and Purification Technology*. 78: 208-213.

[11] Khan, M. M., Filiz, V., Bengtson, G., Shishatskiy, S., Rahman, M.M., Lillepaerg, J., & Abetz, V. 2013. Enhanced Gas

Permeability By Fabricating Mixed Matrix Membranes Of Functionalized Multiwalled Carbon Nanotubes And Polymers Of Intrinsic Microporosity (PIM). *Journal of Membrane Science*. 436: 109-120.

[12] Kim, S., Chen, L., Johnson, J. K., & Marand, E. 2007. Polysulfone And Functionalized Carbon Nanotube Mixed Matrix Membranes For Gas Separation: Theory And Experiment. *Journal of Membrane Science*. 294: 147-158.

[13] Ackerman, D. M., Skoulidas, A. I., Sholl, D. S., & Karl Johnson, J. 2003. Diffusivities of Ar and Ne in Carbon Nanotubes. *Molecular Simulation*. 29: 677-684.

[14] Chen, H., Johnson, J. K., & Sholl, D. S. 2006. Transport Diffusion Of Gases Is Rapid In Flexible Carbon Nanotubes. *Journal of Physical Chemistry B*. 110: 1971-1975.

[15] Malikov, E. Y., Muradov, M. B., Akperov, O. H., Eyvazova, G. M., Puskás, R., Madarász, D., Nagy, L., Kukovecz, Á., & Kónya, Z. 2014. Synthesis And Characterization Of Polyvinyl Alcohol Based Multiwalled Carbon Nanotube Nanocomposites. *Physica E: Low-dimensional Systems and Nanostructures*. 61: 129-134.

[16] Jiang, M.-J., Dang, Z.-M., Yao, S.-H., & Bai, J. 2008. Effects Of Surface Modification Of Carbon Nanotubes On The Microstructure And Electrical Properties Of Carbon Nanotubes/Rubber Nanocomposites. *Chemical Physics Letters*. 457: 352-356.

[17] de Lannoy, C.-F., Soyer, E., & Wiesner, M. R. 2013. Optimizing Carbon Nanotube-Reinforced Polysulfone Ultrafiltration Membranes Through Carboxylic Acid Functionalization. *Journal of Membrane Science*. 447: 395-402.

[18] Avilés, F., Sierra-Chi, C. a., Nistal, a., May-Pat, a., Rubio, F., & Rubio, J. 2013. Influence Of Silane Concentration On The Silanization Of Multiwall Carbon Nanotubes. *Carbon*. 57: 520-529.

[19] Cong, H., Zhang, J., Radosz, M., & Shen, Y. 2007. Carbon Nanotube Composite Membranes Of Brominated Poly(2,6-diphenyl-1,4-phenylene oxide) for Gas Separation. *Journal of Membrane Science*. 294: 178-185.

[20] Wong, K. C., Goh, P. S., Ng, B. C., & Ismail, A. F. 2015. Thin Film Nanocomposite Embedded With Polymethyl Methacrylate Modified Multi-Walled Carbon Nanotubes For CO2 Removal. *RSC Adv*. 5: 31683-31690.

[21] Wong, K. C., Goh, P. S., & Ismail, A. F. 2015. Gas Separation Performance Of Thin Film Nanocomposite Membranes Incorporated With Polymethyl Methacrylate Grafted Multi-Walled Carbon Nanotubes. *International Biodeterioration and Biodegradation*. 102: 339-345.

[22] Xia, H., Wang, Q., & Qiu, G. 2003. Polymer-Encapsulated Carbon Nanotubes Prepared through Ultrasonically Initiated In Situ Emulsion Polymerization. *Chemistry of Materials*. 15: 3879-3886.

[23] Wu, H. X., Qiu, X. Q., Cao, W. M., Lin, Y. H., Cai, R. F., & Qian, S. X. Polymer-wrapped Multiwalled Carbon Nanotubes Synthesized Via Microwave-Assisted In Situ Emulsion Polymerization And Their Optical Limiting Properties. *Carbon*. 45: 2866-2872.

[24] Avilés, F., Cauich-Rodríguez, J.V., Moo-Tah, L., May-Pat, A., & Vargas-Coronado, R. 2009. Evaluation Of Mild Acid Oxidation Treatments For MWCNT Functionalization. *Carbon*. 47: 2970-2975.

[25] Dong, C., Campell, A. S., Eldawud, R., Perhinschi, G., Rojanasakul, Y., & Dinu, C. Z. 2013. Effects Of Acid Treatment On Structure, Properties And Biocompatibility Of Carbon Nanotubes. *Applied Surface Science*. 264: 261-268.

[26] Sahoo, N. G., Rana, S., Cho, J. W., Li, L., & Chan, S. H. 2010. Polymer Nanocomposites Based On Functionalized Carbon Nanotubes. *Progress in Polymer Science*. 35: 837-867.

[27] Jimenez-Solomon, M. F., Gorgojo, P., Munoz-Ibanez, M., & Livingston, A. G. 2013. Beneath The Surface: Influence Of Supports On Thin Film Composite Membranes By Interfacial Polymerization For Organic Solvent Nanofiltration. *Journal of Membrane Science*. 448: 102-113.

[28] Ghosh, A. K., Jeong, B. H., Huang, X., & Hoek, E. M. V 2008. Impacts Of Reaction And Curing Conditions On Polyamide Composite Reverse Osmosis Membrane Properties. *Journal of Membrane Science*. 311: 34-45.

[29] Baroña, G.N.B., Lim, J., Choi, M., & Jung, B. 2013. Interfacial Polymerization Of Polyamide-Aluminosilicate SWNT Nanocomposite Membranes For Reverse Osmosis. *Desalination*. 325: 138-147.

[30] Ge, L., Wang, L., Du, A., Hou, M., Rudolph, V., & Zhu, Z. 2012. Vertically-aligned Carbon Nanotube Membranes For Hydrogen Separation. *RSC Advances*. 2: 5329.

[31] Ge, L., Zhu, Z., & Rudolph, V. 2011. Enhanced Gas Permeability By Fabricating Functionalized Multi-Walled Carbon Nanotubes And Polyethersulfone Nanocomposite Membrane. *Separation and Purification Technology*. 78: 76-82.

[32] Shen, J. N., Yu, C. C., Ruan, H. M., Gao, C. J., & Van der Bruggen, B. 2013. Preparation And Characterization Of Thin-Film Nanocomposite Membranes Embedded With Poly(Methyl Methacrylate) Hydrophobic Modified Multiwalled Carbon Nanotubes By Interfacial Polymerization. *Journal of Membrane Science*. 442: 18-26.

[33] Goh, P.S.S., Ng, B.C.C., Ismail, A.F.F., Aziz, M., & Hayashi, Y. 2012. Pre-treatment of Multi-Walled Carbon Nanotubes For Polyetherimide Mixed Matrix Hollow Fiber Membranes. *Journal of Colloid and Interface Science*. 386: 80-87.

[34] Yong, H. H., Park, H. C., Kang, Y. S., Won, J., & Kim, W. N. 2001. Zeolite-filled Polyimide Membrane Containing 2,4,6-Triaminopyrimidine. *Journal of Membrane Science*. 188: 151-163.